Correlation Analysis of Seasonal Changes on Aerosol Concentration Using Remote Sensing in Java Island

G A Muhammad[1,*], A Amaanah[1], and V C K Dewi

[1] Universitas Pendidikan Indonesia

*Corresponding author's email: gardaasamuhammad@upi.edu

Abstract. Aerosols are small particles in the atmosphere that affect the climate through direct and indirect mechanisms. Aerosols can influence the climate and play a role in cloud formation and precipitation. This study aims to analyze the relationship between seasonal changes and aerosol concentrations, and to identify parameters that influence aerosol concentrations in Java Island using remote sensing. The method used in this study is the Pearson correlation test to determine the relationship between seasonal changes and aerosol concentrations in the atmosphere. The results show that there is a relationship between Aerosol Optical Depth (AOD) and rainfall with a correlation value (R) of 0.8. This result indicates a significant relationship between the two variables. Meanwhile, the analysis results between Aerosol Optical Depth (AOD) and wind speed show a correlation value (R) of 0.05. This result indicates that the relationship between Aerosol Optical Depth (AOD) and wind speed is very weak between the two variables.
Keyword: Aerosol, Pearson Correlation Test, Seasonal Changes.

1. Introduction

Aerosols are small particles in the atmosphere that affect the climate through direct mechanisms (absorbing and scattering radiation) and indirect mechanisms (acting as cloud condensation nuclei and ice nuclei, influencing cloud albedo, precipitation efficiency, and the hydrological cycle) [1]. By definition, aerosols in the atmosphere can influence the climate by scattering and absorbing solar radiation, as well as playing a role in cloud formation and precipitation. Chemically, aerosols are sites for various reactions that can produce new particles or alter the composition of the atmosphere. In addition, aerosol concentration is influenced by seasonal cycles that can be caused by certain factors.

Fluctuations in aerosol concentrations often occur throughout the year. Aerosol concentrations tend to increase during the dry season (May to August) with low rainfall and many calm winds (<1 m/s), causing pollutants to be trapped in the atmosphere. Conversely, concentrations decrease during the rainy season (December to February) due to rain acting as an air cleaner (rain wash), depositing particles from the atmosphere. Weather factors such as wind speed and temperature also play a role, where high wind speeds help disperse pollutants, while low temperatures in the morning cause particles to be denser and more difficult to disperse [2].

Aerosols can contribute to air quality in an area, which significantly impacts human health. These aerosol particles come from various sources such as motor vehicles, industry, and other activities. These particles are very small in size, so they can be inhaled and enter the respiratory system. Epidemiological studies have shown a relationship between exposure to particles in µg/m3 units and their impact on human health. The studies indicate that an increase in aerosol concentration in the air may be associated

with an increased risk of respiratory diseases, cardiovascular disorders, and premature death. In addition, aerosols contribute to phenomena such as acid rain, environmental acidification, and a decrease in air quality. Aerosol sources can be natural, such as volcanic dust and sea salt, or anthropogenic, such as industrial pollution and fossil fuel combustion [3].

Remote sensing satellites offer an effective way to monitor aerosols in the atmosphere. Remote sensing can be used for aerosol analysis through observations of Aerosol Optical Depth (AOD), which measures the concentration and distribution of aerosols in the atmosphere. MODIS (Moderate Resolution Imaging Spectroradiometer) is used for aerosol detection by observing Aerosol Optical Depth (AOD) through algorithms based on surface reflectance and atmospheric scattering. MODIS provides daily global coverage with high spatial resolution (10 km to 3 km), enabling analysis of aerosol distribution on a broad scale, including fine particles ($PM_{2.5}$). This data supports air quality monitoring, climate change research, and the detection of events such as dust storms or forest fires [4].

Previous research on the correlation between aerosol concentration and seasonal changes using remote sensing has shown that seasonal variations in aerosol concentrations, such as $PM_{2.5}$ and optical aerosols, are strongly influenced by atmospheric factors and emission sources that differ in each season. For example, Pathak et al. explained that variations in black carbon (BC) concentrations occur due to differences in atmospheric boundary layer (ABL) depth caused by different solar heating at the Earth's surface, as well as differences in aerosol source strength and production in various seasons [5]. This research shows that an increase in BC concentration in the afternoon is related to increased household activities and the formation of surface inversions that inhibit vertical mixing in the atmosphere.

In addition, research by Lin et al. highlights interannual and seasonal variations in aerosol characteristics, showing that aerosol measurements from remote sensing can provide important insights into how aerosol characteristics change over time and seasons [6]. This study emphasizes the importance of continuous aerosol monitoring to understand seasonal impacts on air quality and human health.

In the context of remote sensing, the use of data from satellites such as MODIS and MISR is very important to estimate $PM_{2.5}$ concentrations and optical aerosols. Lee et al. showed that there is good agreement between $PM_{2.5}$ concentrations measured on-site and those predicted using satellite data, indicating that remote sensing can improve our ability to assess $PM_{2.5}$ exposure in cross-sectional studies [7]. In addition, Dey and Tripathi noted that remote sensing of aerosols provides broad and continuous information on aerosol distribution in various regions, which is very useful for understanding seasonal patterns [8].

The correlation between aerosols and seasonal changes is also seen in research conducted by Sharif et al., who found that high values of aerosol optical depth (AOD) occur during the monsoon season, indicating that certain meteorological conditions can significantly affect aerosol concentrations [9]. This study emphasizes the importance of air trajectory modeling to understand aerosol sources and distribution during various seasons.

Overall, these studies indicate that remote sensing is a highly valuable tool in understanding aerosol dynamics and their impact on air quality, especially in the context of seasonal changes. By utilizing data from various satellites, researchers can gain a clearer picture of how aerosols behave in the atmosphere and how they interact with other environmental factors.

In this context, the aim of this study is to analyze the relationship between seasonal changes and aerosol concentrations and to identify parameters that influence aerosol concentrations in Java Island. By utilizing remote sensing, this study is expected to provide a more comprehensive understanding of the fluctuations in aerosol concentrations that occur throughout the year, as well as the factors that contribute to these changes. The results of this study will not only enrich scientific understanding but can also serve as a basis and reference for the government to determine more effective policies in managing air quality and mitigating its impacts on public health.

2. Research Method

2.1. Study Area

The research location focuses on the entire area of Java Island as can be seen in Figure 1. Java Island is one of the islands in Indonesia, geographically located between 6°-11° S and 95°-106° E. Java Island is bordered by seas, with the Java Sea to the north and the Indian Ocean to the south. The island has six provinces, namely DKI Jakarta Province, Banten Province, West Java Province, DIY Yogyakarta Province, Central Java Province, and East Java Province.

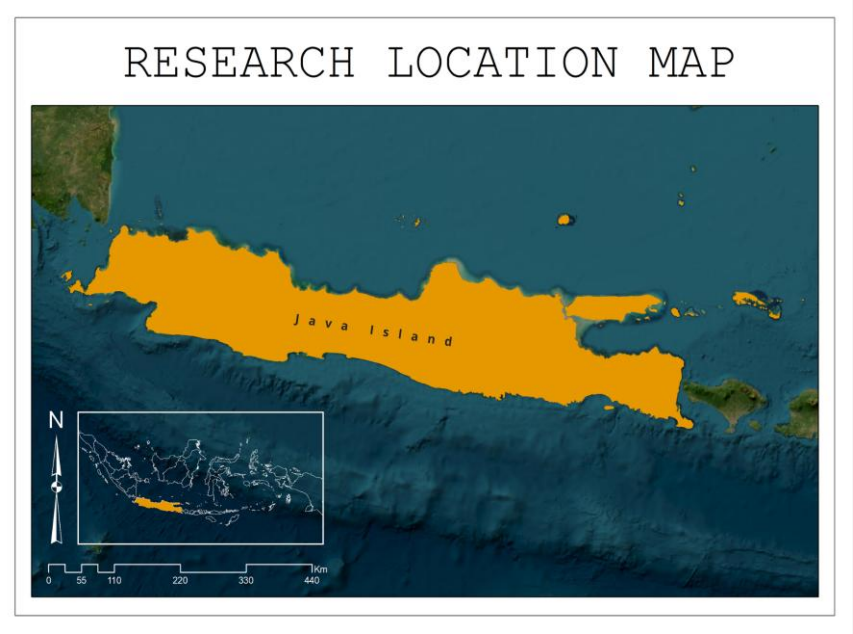

Figure 1. Study Area.

2.2. Data

The data used in this study can be seen in table 1 that consists of MODIS satellite imagery, wind speed, and monthly rainfall. The administrative boundaries of Java Island serve as supporting data in this study as the research area limits. Each dataset is collected in a time series from January to November 2024.

Table 1. Data used in this study.

No.	Data	Spatial Resolution	Temporal	Reference
1.	MODIS *Aerosol Optical Depth* (AOD)	Raster – 1 km	1-2 days	[10]
2.	PERSIANN Dynamic Infrared-Rain Rate (PDIR-Now)	0.04° x 0.04°	daily	[11]
3.	Wind Speed	9x9 km	15 days	[12]
4.	Administrative Data	Vector (1:250.000)	-	[13]

1) MODIS Aerosol Optical Depth (AOD)
   MODIS (Moderate Resolution Imaging Spectroradiometer) is a sensor installed on the Terra and Aqua satellites owned by the National Aeronautics and Space Administration (NASA). One of the products generated from this sensor is MODIS Aerosol Optical Depth (AOD), which is used to monitor the concentration of aerosol thickness in the atmosphere with a resolution of 1 km. MODIS AOD utilizes the Multi-Angle Implementation of Atmospheric Correction (MAIAC) algorithm in processing information on aerosol concentration thickness [10].

2) Precipitation
   Precipitation data was used to map rainfall levels in the study area during March, August, and November 2024 and its correlation with aerosol concentrations in the atmosphere. Precipitation data was obtained through the PERSIANN Dynamic Infrared-Rain Rate (PDIR-Now) by interpolating rainfall estimates in the study area.
3) Wind Speed
   Wind speed data was used to map wind speeds in the study area during the periods of March, August, and November 2024, and was also used to determine its correlation with aerosol concentrations in the atmosphere. Wind speed values were obtained from the European Centre for Medium-Range Weather Forecasts (ECMWF) by interpolating wind speed values during the specified time periods.
4) Administrative Data
   Administrative boundary data is important data used as the boundary of the study area in research. In this study, the administrative data for the island of Java was sourced from the Geospatial Information Agency (BIG).

2.3. Data Processing Techniques

The full flowchart can be seen in figure 2. The activities begin with selecting the location as the initial stage of the research, followed by data acquisition. The main data acquisition includes MODIS Aerosol Optical Depth (AOD) data from GEE, rainfall data from CHRS, and wind speed data from ECMWF ERA5. In the data processing stage, the work is divided into two parts, namely data processing for accuracy testing and for mapping.

The results of the first-stage accuracy test processing for MODIS Aerosol data, rainfall data, and wind speed data are then processed to calculate the average for each month from January to November 2024. Each main dataset is then converted into a time series from the average of each dataset, namely the time series for rainfall, the time series for aerosols, and the time series for wind speed. Once the time series of the main data is obtained, the next step is to perform correlation tests divided into two parts. The correlation test is conducted for aerosol and rainfall correlation and aerosol and wind speed correlation, resulting in two correlation graphs.

We implemented the correlation analysis by extracting pixel values from each monthly image onto a common set of sampling points, and then computing Pearson correlations at each point. The procedure and quality-control steps are described below:

1. Spatial alignment and sampling grid
   All raster inputs (MODIS MAIAC AOD, PERSIANN precipitation, ERA5 u/v) were first reprojected to a common geographic coordinate system (WGS84) and inspected for consistent spatial extent and orientation. We defined a regular sampling grid of point locations at the centre of each target grid cell (recommended: 0.04° × 0.04°) covering the whole island of Java. Using a single sampling-point grid ensures a one-to-one spatial correspondence between extracted values and simplifies pixel-wise comparison across datasets.
2. Monthly aggregation and quality filtering
   Daily-level data were aggregated to monthly means before extraction to reduce short-term noise and to match the seasonal objective. For the MODIS AOD product we applied the recommended

QA filter and removed cloud-contaminated retrievals. For each month and for each sampling point we recorded the number of valid daily observations used to compute the monthly mean; points with fewer than five valid daily observations in a month were treated as missing for that month. Similarly, any monthly cell in other datasets with insufficient observations was flagged as missing.

3. Extracting pixel values to points
   For each monthly raster (AOD, rainfall, u, v), we extracted the raster value at each sampling point. Continuous fields (AOD, u, v, rainfall) were extracted using bilinear interpolation from the gridded raster to the point locations when the raster and sampling-grid cell centers did not align exactly; nearest-neighbour extraction was used only when preserving original pixel values was required. For wind, the u and v components were extracted separately at each point and wind speed was computed afterward as sqrt(u^2 + v^2) .
4. Building point-wise time series
   After extraction we constructed a monthly time series for each sampling point consisting of the monthly AOD, rainfall, and wind-speed values over the study period (January–November 2024, N = 11). Only months where both variables were valid contributed to the correlation pair for that point. We recorded the number of valid months per point and excluded points with fewer than six valid months from the pixel-wise correlation analysis to avoid unstable estimates.
5. Pearson correlation and inference at each point
   For each sampling point we computed the Pearson correlation coefficient r between the monthly AOD series and the monthly rainfall series (and separately between AOD and wind speed). The significance of r was assessed using the Student's t-transform with degrees of freedom N_eff-2, where N_eff is the number of valid paired months at that point. To account for possible temporal autocorrelation in the short monthly series, we estimated lag-1 autocorrelations for each variable at representative regions and, where warranted, applied an effective sample-size correction N_eff = N * (1 - rho1*rho2) / (1 + rho1*rho2) (with rho1 and rho2 the lag-1 autocorrelations of the two series). Confidence intervals for r were computed using Fisher's z-transform.

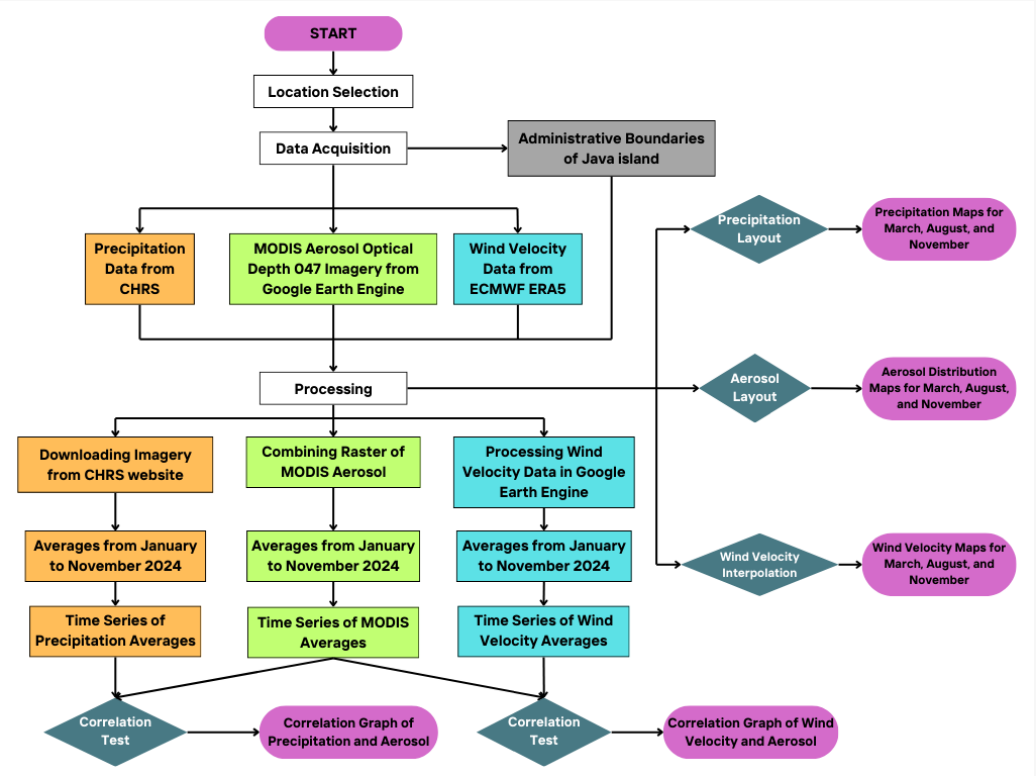

Figure 2. Research Flow Diagram.

3. Result and Discussion

3.1. Rainfall in 2024 on Java Island

The monthly rainfall time series figure 3 shows two clear peaks during 2024: the primary peak occurred in March (maximum monthly rainfall ≈ 450 mm) and a secondary increase in November; the dry season minima occurred between April and September with the lowest rainfall in August. The spatial rainfall maps for March, August, and November figure 4 reflect these temporal patterns: March exhibits widespread high rainfall (>300 mm across most provinces), August displays widespread dry conditions (0–100 mm in most areas), and November shows renewed rainfall in many regions consistent with the onset of the wet season.

This rainfall pattern represents the occurrence of two seasons in Indonesia, where the rainy season occurs from January to March and October to November, characterized by high rainfall. The dry season occurs from April to September, marked by very low rainfall, with the lowest peak in August.The end of the rainy season is marked by the transition from March to April, which shows a significant decrease in rainfall. Meanwhile, the spike in rainfall from October to November indicates the start of the rainy season again.

Based on the graph, the provinces with the highest average rainfall are Banten and DKI Jakarta, while the provinces with the lowest average rainfall are Central Java and East Java. High rainfall in Banten and DKI Jakarta can be attributed to their location near the west coast of Java Island and the influence of the west monsoon winds that carry abundant water vapor. Conversely, Central Java and East Java tend to be drier due to the rain shadow effect and the dominance of dry winds from Australia at certain times. In addition, local factors such as urbanization and topography also play a major role.

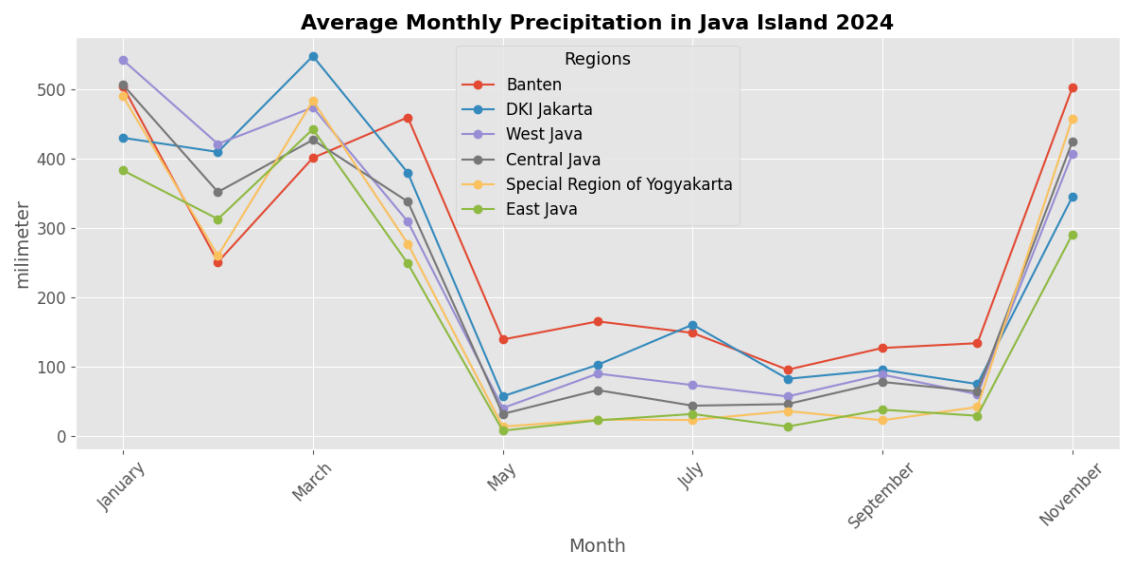

Figure 3. Average rainfall graph on Java Island

The map in figure 4 is a visualization of rainfall in 2024 represented by the months of March, August, and November 2024. These three months were chosen because these months correspond to distinct seasonal phases in 2024 (see figures 3–4): March is the primary rainy-season peak (highest monthly rainfall), August represents the dry-season minimum rainfall and maximum persistence of dry conditions, and November marks the onset of the second rainy-season peak as rainfall increases again. Choosing these three months therefore captures the key hydrometeorological states (wet peak, dry trough, and wet onset) that are expected to drive changes in aerosol loading and transport across Java.

Using the three seasonal snapshots also facilitates direct visual comparison of AOD, rainfall, and wind fields at representative points in the annual cycle while keeping the mapping and interpretation tractable.

Rainfall levels are classified into four classes: 0-100 mm (dark green), 100-300 mm (light green), 300-500 mm (yellow), and >500 mm (red). This classification refers to the normal monthly rainfall classification of the Meteorology, Climatology, and Geophysics Agency. In March, high rainfall levels ranged from 300 to >500 mm. Almost all provinces on Java Island had rainfall >500 mm. Only Banten Province had rainfall between 300-500 mm. This month shows that the peak of the rainy season in 2024 occurred in March.

August is the peak of the dry season with dry conditions in almost all areas. Rainfall intensity only ranged from 0-300 mm. The eastern part of Banten, the western part of West Java, and the southern part of DKI Jakarta experienced rainfall of 100-300 mm. Meanwhile, other areas experienced very low rainfall intensity, which was 0-100 mm. In November, rainfall with an intensity of 100 to >500 mm (yellow to red) began to appear in various regions. Meanwhile, dark green (0-100 mm) began to disappear and was only found in the eastern part of Java Island. This indicates that rainfall was increasing again, marking the start of the rainy season.

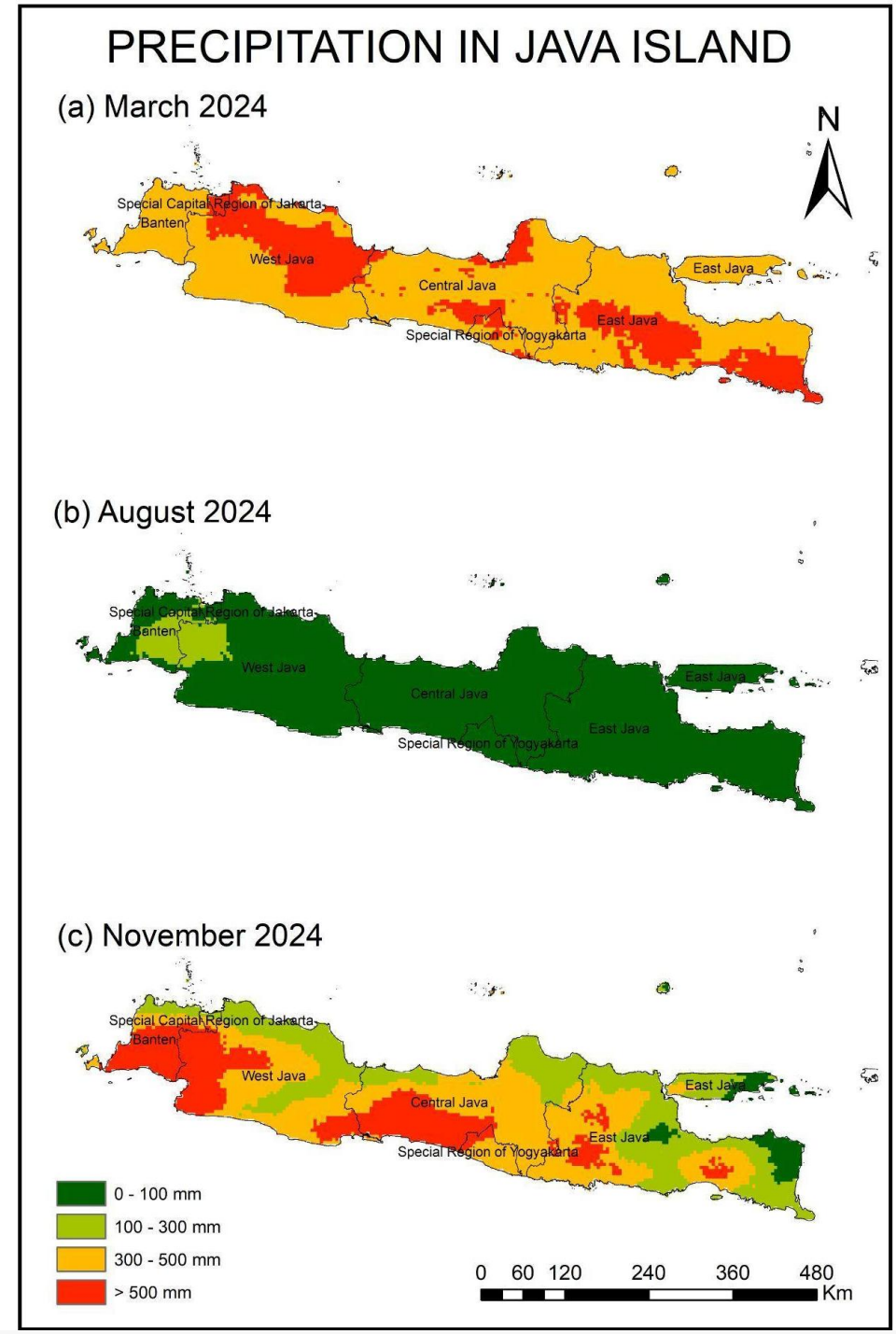

Figure 4. Rainfall map of Java Island 2024.

3.2. Wind Speed in March, August, and November 2024

The wind direction map was obtained from ERA 5 ECMWF data processed using the Google Earth Engine platform and produced an average wind speed map for March, August, and November on Java Island as follows. The map shown in figure 5 is a visualization of the results of processing average wind speed on Java Island in March, August, and November 2024. The data used is wind speed data from ECMWF ERA 5 acquired through Google Earth Engine.

Wind speed levels are divided into 5 classes with wind speed units in m/s. These wind speed classes consist of 0-0.2 m/s visualized with dark purple with 0.02 m/s being the lowest wind speed value in the data used, 0.3-1.5 m/s in light purple, 1.6-3.3 m/s in red, 3.4-5.4 m/s in orange, and >5.5 m/s in yellow with 7.432 m/s as the highest speed level in the data used. Average wind speed maps in figure 5 show higher wind speeds in coastal zones and along the southern coast facing the Indian Ocean. Temporal series figure 6 indicate the highest monthly mean wind speeds in August, particularly over southern Java and Yogyakarta, likely driven by regional circulation changes during the dry season.

In March 2024, the average wind speed on Java Island was in a varied range. Wind speeds of >5.5 m/s were mostly found in coastal areas of Java Island, especially on the north coast. Meanwhile, wind speeds in the range of 0.3-5.4 m/s dominated Banten Province, DKI Jakarta, and West Java. The provinces of Central Java and East Java had average wind speeds in the range of 0.2-5.4 m/s.

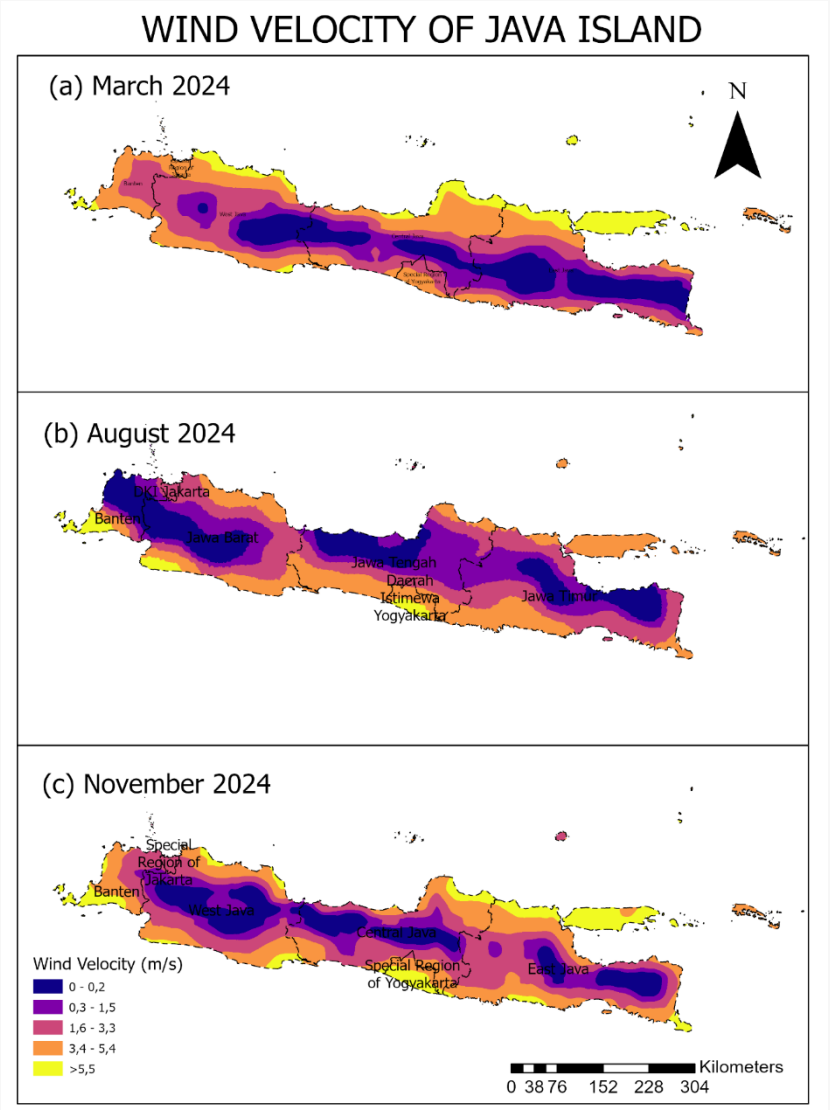

Figure 5. Average wind speed map of Java Island 2024.

In August 2024, low average wind speeds dominated Banten, DKI Jakarta, and West Java provinces in the range of 0-3.3 m/s, and the southern coastal parts of Banten and West Java had higher wind speeds. Central Java and East Java provinces were dominated by average wind speeds of 0.2-5.4 m/s. The Special Region of Yogyakarta was dominated by wind speeds of 1.6-5.4 m/s, and there were areas with high wind speeds >5.5 m/s concentrated in the southern part.

In November 2024, the average wind speed was observed to be higher than in August. Almost all coastal areas, whether north, south, west, or east, had high average wind speeds up to >5.5 m/s. The provinces of Banten, DKI Jakarta, and the Special Region of Yogyakarta had higher wind speeds compared to other regions on Java Island, in the range of 1.6-5.4 m/s. West Java and Central Java provinces were dominated by low to moderate wind speeds ranging from 0.2-3.3 m/s. Meanwhile, the average wind speed in East Java Province was in the moderate to high range, from 0.3-5.4 m/s. The following is a time series result of average wind speed on Java Island from January to November 2024.

Based on the graph in figure 6, the highest peak wind speed from January to November 2024 was in August, with the region having the highest wind speed being the Special Region of Yogyakarta. The factor causing high wind speeds in the Special Region of Yogyakarta is its location in the southern part, directly bordering the Indian Ocean. The southern sea of Java Island compared to the northern, western, and eastern seas is more dynamic, so its wind friction patterns are relatively stable.

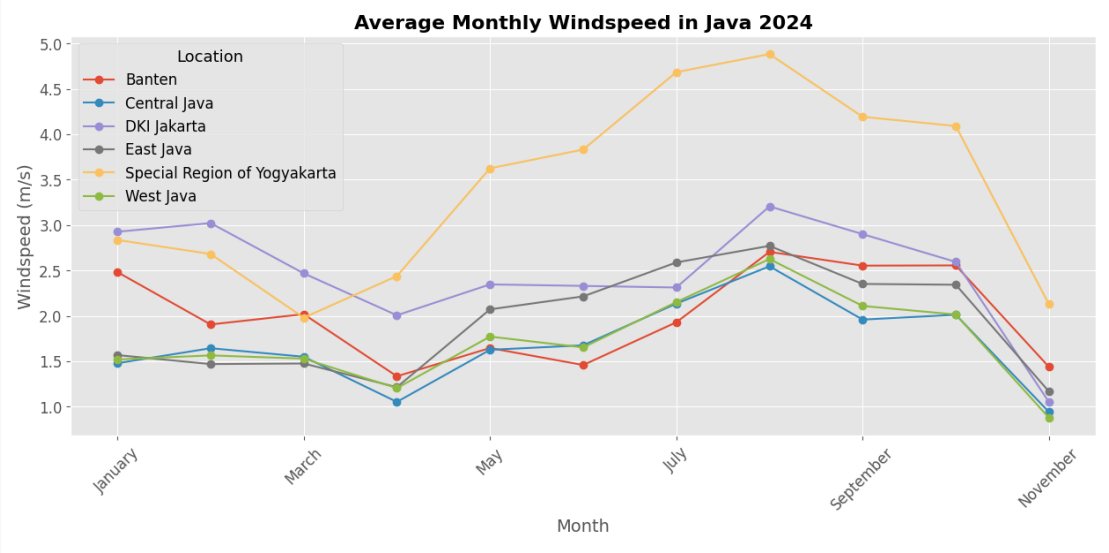

Figure 6. Average wind speed graph of Java Island 2024

3.3. MODIS Satellite Aerosol Concentration Map

Based on the time series analysis graph in figure 7 showing the monthly average Aerosol Optical Depth (AOD) in several regions on Java Island in 2024, there was a significant increase in May, especially in DKI Jakarta and Banten. This increase can be linked to the seasonal transition on Java Island, where in May, the region transitions from the rainy season to the dry season. During this transition period, changes in monsoon wind direction can carry aerosol pollutants from local and regional sources, contributing to the increase in AOD [14]. In addition, human activities such as biomass burning, motor vehicle use, and industrial activities also play an important role in increasing aerosol concentrations in the atmosphere [15], [16].

DKI Jakarta, as one of the regions with a high level of urbanization and significant population density, showed the highest AOD spike compared to other regions. This can be explained by the high pollutant emissions from the transportation and industrial sectors in the area [16]. Research shows that aerosol emissions from human activities, especially in urban areas, can increase aerosol concentrations that affect air quality [15], [16]. Banten, which is close to Jakarta, also experienced an increase in AOD, most likely influenced by local contributions from intensive economic and transportation activities [14].

After peaking in May, aerosol concentrations generally decreased gradually until the end of the year. This shows the influence of factors such as changes in wind patterns, increased rainfall during the rainy season, and efforts to mitigate aerosol particle emissions. High wind speeds can cause wider dispersion of aerosol particles, thus reducing aerosol concentrations in an area. However, winds that are too strong can also lift dust particles from the surface, increasing aerosol concentrations. Meanwhile, rainfall acts

as a cleaning process of the atmosphere from aerosol particles. Raindrops capture and carry aerosol particles to the earth's surface, thereby reducing AOD values.

The variation in aerosol concentrations between regions on Java Island is also quite significant. Banten and DKI Jakarta show a similar pattern, with sharper increases compared to other regions. This indicates the presence of similar emission sources, such as dense industrial and transportation activities in the Jabodetabek area.

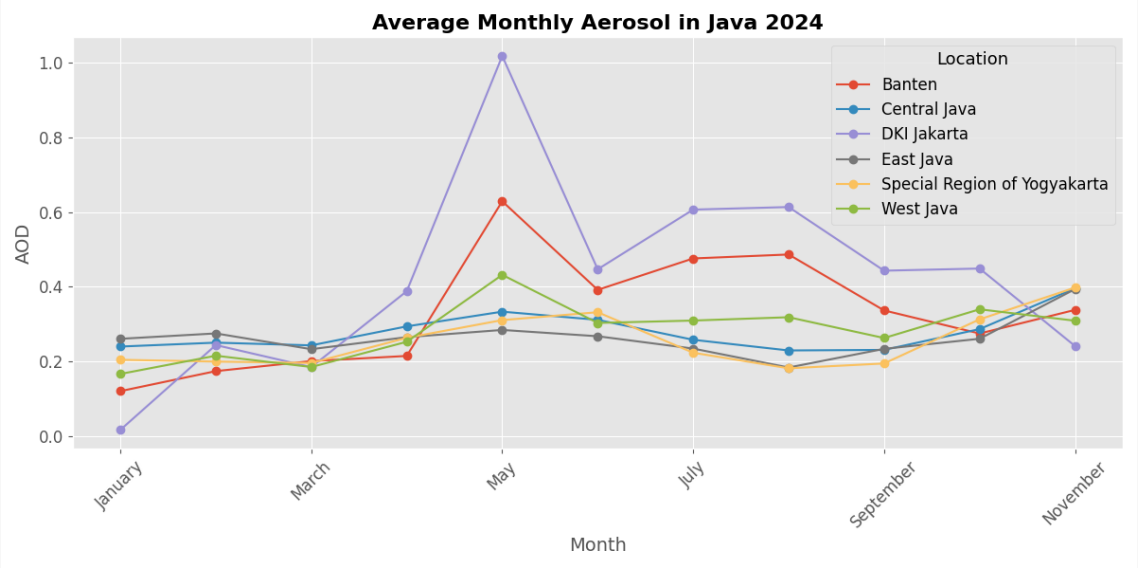

Figure 7. Average aerosol concentration graph of Java Island 2024.

The map in figure 8 is an Aerosol Optical Depth map from MODIS imagery data processed using the Google Earth Engine (GEE) platform, using imagery data from 2024. The time series used as comparison data are for March, August, and November. These data are used to see the effect of AOD during seasonal changes on Java Island itself.

The value range used was adjusted to the highest value in the selected months, in this case, November, with a maximum value of 2.13. After reclassifying the values for other months, the visualization produced appears as shown on the map above. The color visualization from lowest to highest starts from dark blue with a value of 0-0.32, turquoise 0.32-0.48, light green 0.48-0.73, orange 0.73-1.08, and the highest is red with a value range of 1.08-2.13.

In March, low aerosol concentrations were seen because March is still in the rainy season, but the northern part had moderate aerosol concentrations, which could be influenced by various factors. In August, which is the dry season or the peak of the dry season, aerosol concentrations began to increase from the west. During the dry season, winds usually blow from west to east, carrying aerosol particles from more polluted areas to other regions on Java Island. This causes aerosol concentrations to increase in the east along with the movement of these particles.

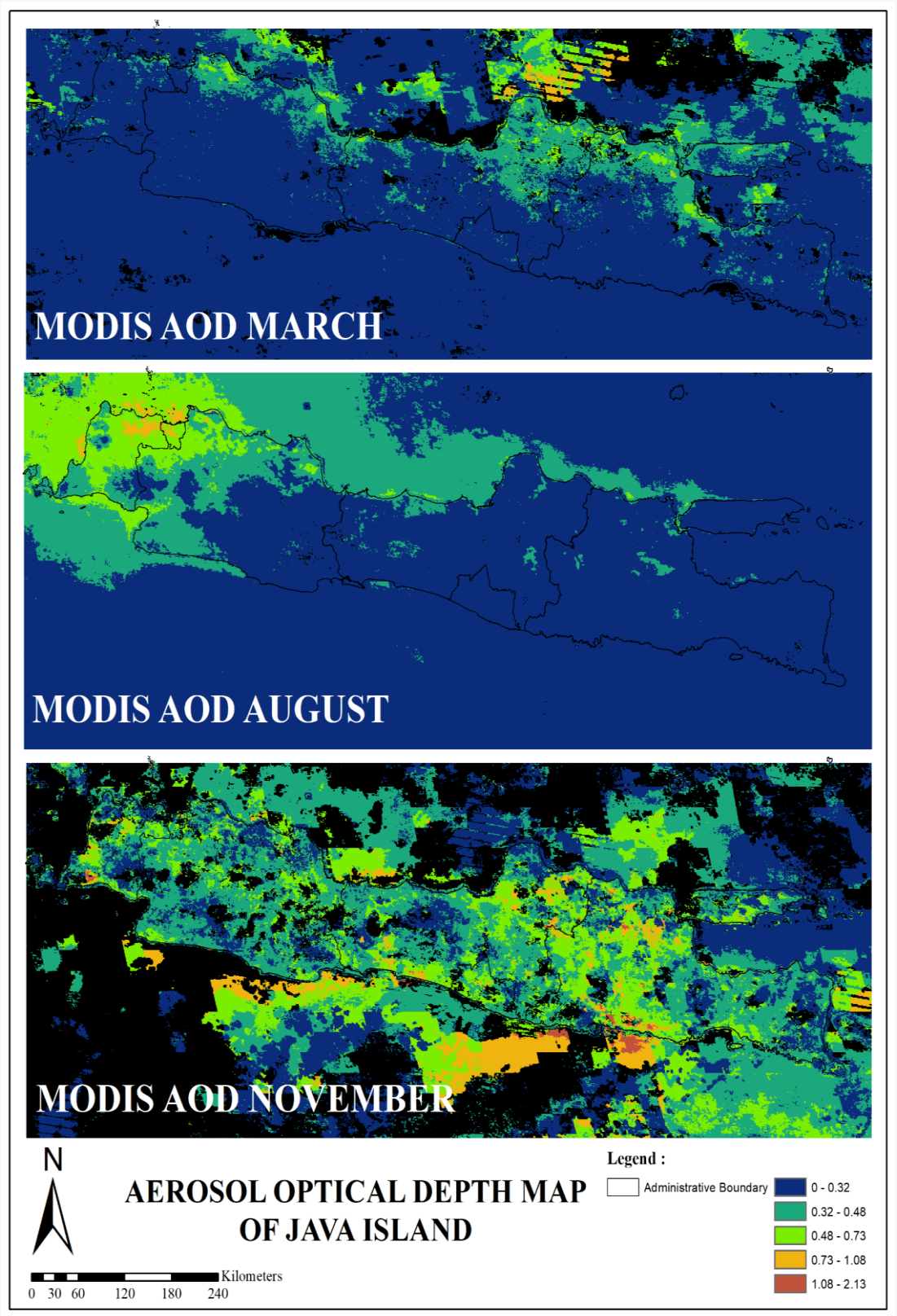

Figure 8. Average aerosol concentration graph of Java Island 2024.

However, in November, aerosol concentrations were quite varied, from low to high, spread evenly across Java Island, even though November is the beginning of the rainy season. This can occur because aerosol concentrations do not immediately decrease or be completely washed away by atmospheric cleaning from rainwater. Several factors influence this, such as the density of the aerosol itself, the concentration level of the aerosol, and the altitude of the aerosol in the atmosphere, which affects how quickly the aerosol settles and decreases. The heavier its mass, the faster it will be washed away by rainwater. The lower the altitude of the aerosol in the atmosphere, the easier it will be to be washed away, unlike higher altitudes, which usually take longer. The concentration level of aerosols this month is also due to the accumulation of aerosols from the previous dry season, so this visualization is normal. In addition, natural phenomena and human activities are also factors that cause an increase in aerosol concentration on Java Island itself.

3.4. Correlation Test Graph Between Aerosol and Rainfall on Aerosol Concentration

The analysis in figure 9 is conducted using the Pearson model shows that there is a strong relationship between Aerosol Optical Depth (AOD) and rainfall, with a correlation value (R) of 0.8. This result indicates a significant relationship between the two variables. Previous studies also support this finding, where correlation analysis shows that an increase in AOD is associated with an increase in rainfall, especially in areas influenced by aerosols that act as condensation nuclei [17], [18], [19] . From the analysis results graph, it can be seen that the higher the rainfall value, the higher the tendency of the AOD value, which is in line with studies showing that aerosols can increase the number of condensation nuclei, thus facilitating the formation of clouds and rainfall [20], [21] .

Aerosols, which consist of small particles such as dust, smoke, and other pollutants, play an important role in the cloud formation process. These aerosol particles act as condensation nuclei, which are the starting point where water vapor in the atmosphere condenses to form cloud droplets. Studies show that in areas with high AOD, there is a significant increase in rainfall due to the large number of condensation nuclei that support an intensive cloud formation process [22], [23]. This finding strengthens the understanding of the relationship between the presence of aerosols in the atmosphere and rainfall dynamics in an area. In addition, the interaction between aerosols and clouds can affect the microphysical properties of clouds, which in turn can influence the rainfall process [24].

Furthermore, research shows that variations in aerosol concentrations can affect convection processes and cloud formation, contributing to different rainfall patterns in various regions [25], [26]. For example, in some areas, an increase in AOD may be associated with an increase in rainfall, but in other areas, this effect may be the opposite, depending on meteorological conditions and the nature of the aerosols present [27], [28]. Therefore, it is important to consider local context and other meteorological factors when analyzing the relationship between AOD and rainfall.

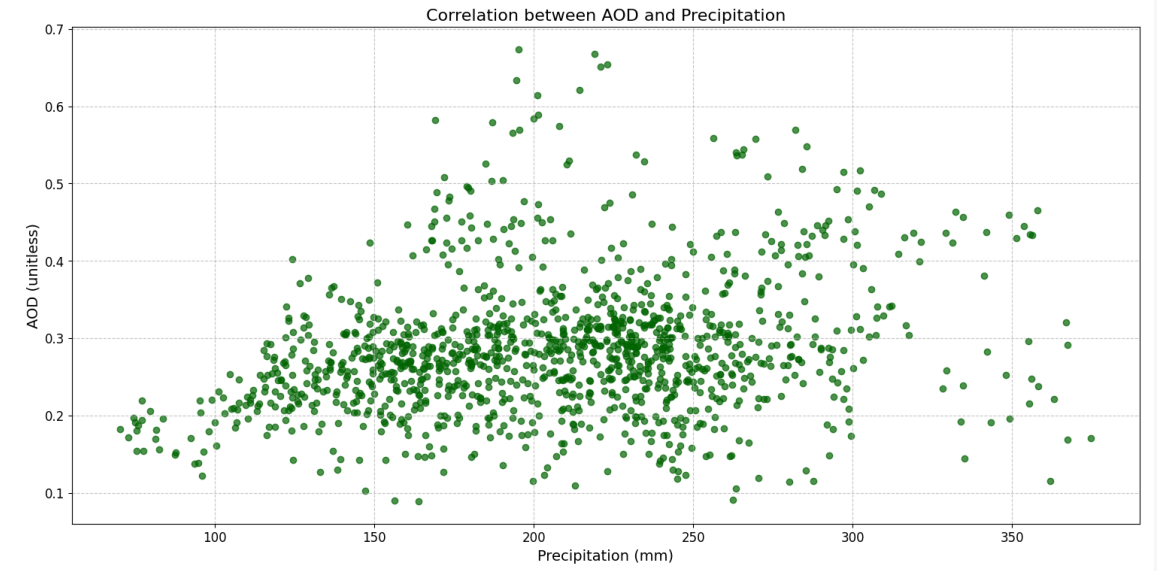

Figure 9. AOD and rainfall correlation test.

3.5. Correlation Test Graph Between Aerosol and Wind Speed on Aerosol Concentration

Based on the Pearson correlation analysis between wind speed and Aerosol Optical Depth (AOD) as can be seen in figure 10, the results show a correlation value (R) of 0.055, indicating a very weak relationship between the two variables. This value is close to zero, which statistically indicates that there is no significant relationship or clear pattern of correlation between wind speed and AOD in the study area. This is consistent with previous findings showing that although wind speed can affect aerosol distribution, other factors such as aerosol emission sources and atmospheric conditions have a greater influence on AOD values [29], [30].

Further analysis of the scatterplot shows that the distribution of data points is randomly scattered without a clear linear pattern. This supports the conclusion that variations in AOD values do not consistently increase or decrease with changes in wind speed. Previous studies have also noted that although there is a relationship between wind speed and aerosols, this relationship is often influenced by other variables, such as meteorological conditions and different aerosol sources [31], [32]. For example, in cleaner areas, aerosol emissions from sea spray can be the main contributor to AOD, but in more polluted areas, local emission sources can dominate [29], [30].

Physically, these results can be explained by considering that wind speed does affect the distribution of aerosols in the atmosphere, but is not sufficient to explain overall AOD variations. Other processes such as particle deposition, aerosol-cloud interactions, and meteorological variability play a more dominant role in determining AOD values [33], [34]. For example, research shows that aerosols can affect cloud properties and rainfall patterns, which in turn can affect AOD [35], [36]. Therefore, further analysis is needed to understand other factors contributing to AOD values in this region, including the influence of specific aerosol types and more complex atmospheric processes [22], [37].

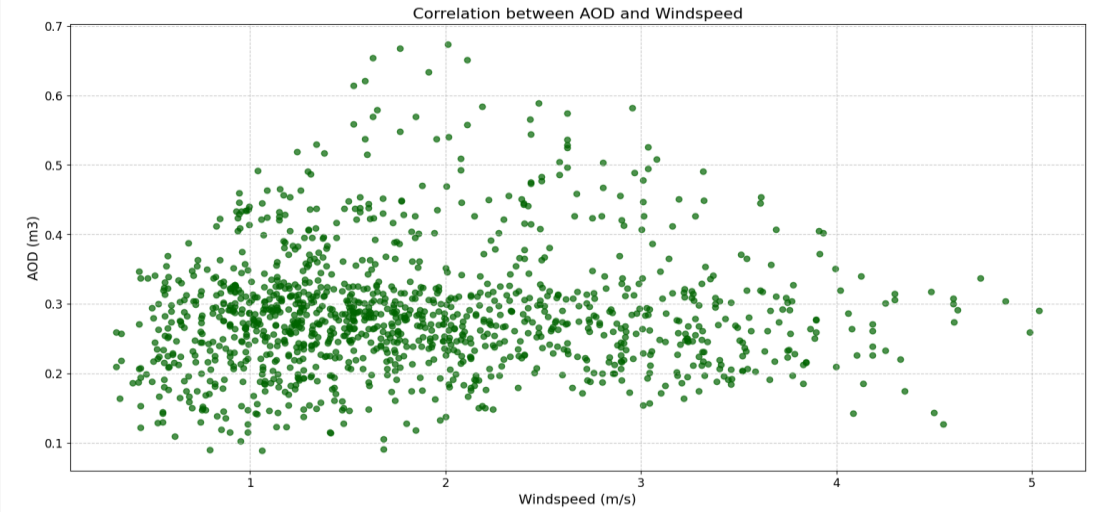

Figure 10. AOD and wind speed correlation test.

4. Conclusion

Based on the results and discussion above, it can be seen that there is a correlation between seasonal changes and aerosol concentrations in the atmosphere. Based on the graph, the parameter that has a strong correlation with aerosol concentrations is rainfall, with a correlation value (R) of 0.8. This is because aerosols act as condensation nuclei. However, this phenomenon can be reversed, depending on meteorological factors and the properties of aerosols in a particular region. Meanwhile, the wind speed parameter has a very weak correlation value of 0.05. This is because variations in AOD values do not consistently increase or decrease with wind speed. This indicates that aerosol distribution does not always depend on wind strength, but is influenced by other factors such as local emission sources and particle characteristics. From this analysis, it is important to consider regional characteristics, aerosol types, and meteorological conditions to understand the dynamics of aerosol concentrations, especially in the context of seasonal changes in a particular region. This is due to the dynamic nature of aerosols, as well as their role as cloud condensation nuclei that affect precipitation, potentially altering the energy balance in the atmosphere by absorbing and reflecting solar radiation. Therefore, their impact on meteorological and climatic conditions is complex and variable. From this analysis, aerosols play a significant role, especially in decision-making regarding air quality management and climate change mitigation. During the dry season, for example, the increase in aerosol concentration caused by reduced rainfall and the intensity of land burning activities needs to be anticipated through the strengthening of regulations restricting open burning and increased monitoring of industrial emissions. A regional approach is also very important to optimize mitigation strategies in accordance with local meteorological characteristics and emission patterns.

References

[1] U. Lohmann dan J. Feichter, "Global indirect aerosol effects: a review," *Atmos. Chem. Phys.*, vol. 5, no. 3, hal. 715–737, 2005, doi: 10.5194/acp-5-715-2005.

[2] S. Gautam, J. Elizabeth, A. Gautam, K. Singh, dan P. Abhilash, "Impact Assessment of Aerosol Optical Depth on Rainfall in Indian Rural Areas," *Aerosol Sci. Eng.*, vol. 6, hal. 186–196, 2022, doi: 10.1007/s41810-022-00134-9.

[3] J. M. Prospero *dkk.*, "The atmospheric aerosol system: An overview," *Rev. Geophys.*, vol. 21, no. 7, hal. 1607–1629, 1983, doi: 10.1029/RG021i007p01607.

[4] S. C. Anenberg *dkk.*, "Using Satellites to Track Indicators of Global Air Pollution and Climate Change Impacts: Lessons Learned From a NASA-Supported Science-Stakeholder Collaborative," *GeoHealth*, vol. 4, no. 7, hal. 1–11, 2020, doi: 10.1029/2020GH000270.

[5] B. Pathak, G. Kalita, K. Bhuyan, P. K. Bhuyan, dan K. K. Moorthy, "Aerosol temporal characteristics and its impact on shortwave radiative forcing at a location in the Northeast of India," *J. Geophys. Res. Atmos.*, vol. 115, no. 19, hal.

1–14, 2010, doi: 10.1029/2009JD013462.
[6] C. Lin, A. K. H. Lau, J. C. H. Fung, X. Q. Lao, Y. Li, dan C. Li, "Assessing the Effect of the Long-Term Variations in Aerosol Characteristics on Satellite Remote Sensing of PM2.5 Using an Observation-Based Model," *Environ. Sci. Technol.*, vol. 53, no. 6, hal. 2990–3000, Mar 2019, doi: 10.1021/acs.est.8b06358.
[7] H. J. Lee, B. Coull, M. Bell, dan P. Koutrakis, "Use of satellite-based aerosol optical depth and spatial clustering to predict ambient PM2.5 concentrations.," *Environ. Res.*, vol. 118, hal. 8–15, 2012, doi: 10.1016/j.envres.2012.06.011.
[8] S. Dey dan S. Tripathi, "Remote Sensing of Atmospheric Aerosols," hal. 119–151, 2014, doi: 10.1002/9781118682555.CH6.
[9] F. Sharif, K. Alam, dan S. Afsar, "Spatio-Temporal Distribution of Aerosol and Cloud Properties over Sindh Using MODIS Satellite Data and a HYSPLIT Model," *Aerosol Air Qual. Res.*, vol. 15, no. 2, hal. 657–672, 2015, doi: 10.4209/aaqr.2014.09.0200.
[10] A. Lyapustin dan Y. Wang, "MODIS/Terra+Aqua Land Aerosol Optical Depth Daily L2G Global 1km SIN Grid V061." NASA Land Processes Distributed Active Archive Center, 2022. doi: 10.5067/MODIS/MCD19A2.061.
[11] P. Nguyen *dkk.*, "The CHRS Data Portal, an easily accessible public repository for PERSIANN global satellite precipitation data," *Nat. Sci. Data*, vol. 6, hal. 180296, 2019, doi: 10.1038/sdata.2018.296.
[12] J. Muñoz Sabater, "ERA5-Land monthly averaged data from 1981 to present." Copernicus Climate Change Service (C3S) Climate Data Store (CDS), 2019. [Daring]. Tersedia pada: https://cds.climate.copernicus.eu/
[13] Badan Informasi Geospasial, "Batas Wilayah Administrasi Provinsi—Layer Area Batas Wilayah Administrasi Provinsi." 2025.
[14] X. Huang dan A. Ding, "Aerosol as a critical factor causing forecast biases of air temperature in global numerical weather prediction models," *Sci. Bull.*, vol. 66, no. 18, hal. 1917–1924, 2021, doi: https://doi.org/10.1016/j.scib.2021.05.009.
[15] U. Abdulkarim dan B. Tijjani, "Effect of Varying Aerosol Concentrations and Relative Humidity on Visibility and Particle Size Distribution in Urban Atmosphere," *J. Atmos. Sci. Res.*, vol. 4, no. 3, hal. 14–28, 2021, doi: 10.30564/jasr.v4i3.3430.
[16] J. Sun *dkk.*, "Measurement report: Long-term changes in black carbon and aerosol optical properties from 2012 to 2020 in Beijing, China," *Atmos. Chem. Phys.*, vol. 22, no. 1, hal. 561–575, 2022, doi: 10.5194/acp-22-561-2022.
[17] S. Han, Y. Li, G. Wen, dan T. Huang, "Study on thermophoretic deposition of micron-sized aerosol particles by direct numerical simulation and experiments," *Ecotoxicol. Environ. Saf.*, vol. 233, hal. 113316, 2022, doi: https://doi.org/10.1016/j.ecoenv.2022.113316.
[18] A. K. Miltenberger *dkk.*, "Aerosol--cloud interactions in mixed-phase convective \hack{\break}clouds -- Part 1: Aerosol perturbations," *Atmos. Chem. Phys.*, vol. 18, no. 5, hal. 3119–3145, 2018, doi: 10.5194/acp-18-3119-2018.
[19] C. M. Naud, D. J. Posselt, dan S. C. van den Heever, "Observed Covariations of Aerosol Optical Depth and Cloud Cover in Extratropical Cyclones," *J. Geophys. Res. Atmos.*, vol. 122, no. 19, hal. 10338–10356, 2017, doi: 10.1002/2017JD027240.
[20] Y. Fan *dkk.*, "Large contributions of biogenic and anthropogenic sources to fine organic aerosols in Tianjin, North China," *Atmos. Chem. Phys.*, vol. 20, no. 1, hal. 117–137, 2020, doi: 10.5194/acp-20-117-2020.
[21] C. Zhou, H. Zhang, S. Zhao, dan J. Li, "On Effective Radiative Forcing of Partial Internally and Externally Mixed Aerosols and Their Effects on Global Climate," *J. Geophys. Res. Atmos.*, vol. 123, no. 1, hal. 401–423, 2018, doi: 10.1002/2017JD027603.
[22] E. Gryspeerdt, P. Stier, dan D. G. Partridge, "Satellite observations of cloud regime development: the role of aerosol processes," *Atmos. Chem. Phys.*, vol. 14, no. 3, hal. 1141–1158, 2014, doi: 10.5194/acp-14-1141-2014.
[23] C. Zhao *dkk.*, "Negative Aerosol-Cloud re Relationship From Aircraft Observations Over Hebei, China," *Earth Sp. Sci.*, vol. 5, no. 1, hal. 19–29, 2018, doi: 10.1002/2017EA000346.
[24] B. S. Grandey, L. K. Yeo, H. Lee, dan C. Wang, "The equilibrium climate response to sulfur dioxide and carbonaceous aerosol emissions from East and Southeast Asia," *Geophys. Res. Lett.*, vol. 45, no. 20, hal. 11–318, 2018.
[25] X. Yang, C. Zhao, L. Zhou, Y. Wang, dan X. Liu, "Distinct impact of different types of aerosols on surface solar radiation in China," *J. Geophys. Res. Atmos.*, vol. 121, no. 11, hal. 6459–6471, 2016.
[26] L. Liu *dkk.*, "Size-dependent aerosol iron solubility in an urban atmosphere," *npj Clim. Atmos. Sci.*, vol. 5, no. 1, hal. 1–6, 2022, doi: 10.1038/s41612-022-00277-z.
[27] S. Namdari, N. Karimi, A. Sorooshian, G. Mohammadi, dan S. Sehatkashani, "Impacts of climate and synoptic fluctuations on dust storm activity over the Middle East," *Atmos. Environ.*, vol. 173, hal. 265–276, 2018, doi: https://doi.org/10.1016/j.atmosenv.2017.11.016.
[28] H. Yan, Z. Li, J. Huang, M. Cribb, dan J. Liu, "Long-term aerosol-mediated changes in cloud radiative forcing of deep clouds at the top and bottom of the atmosphere over the Southern Great Plains," *Atmos. Chem. Phys.*, vol. 14, no. 14, hal. 7113–7124, 2014, doi: 10.5194/acp-14-7113-2014.
[29] S. Dasarathy *dkk.*, "Multi-year seasonal trends in sea ice, chlorophyll concentration, and marine aerosol optical depth in the Bellingshausen Sea," *J. Geophys. Res. Atmos.*, vol. 126, no. 21, hal. e2021JD034737, 2021.
[30] A. Engström dan A. M. L. Ekman, "Impact of meteorological factors on the correlation between aerosol optical depth and cloud fraction," *Geophys. Res. Lett.*, vol. 37, no. 18, 2010.
[31] H. Grythe, J. Ström, R. Krejci, P. Quinn, dan A. Stohl, "A review of sea-spray aerosol source functions using a large global set of sea salt aerosol concentration measurements," *Atmos. Chem. Phys.*, vol. 14, no. 3, hal. 1277–1297, 2014.
[32] F. Niu dan Z. Li, "Systematic variations of cloud top temperature and precipitation rate with aerosols over the global

tropics," *Atmos. Chem. Phys.*, vol. 12, no. 18, hal. 8491–8498, 2012.
[33] L. A. Regayre *dkk.*, "Aerosol and physical atmosphere model parameters are both important sources of uncertainty in aerosol ERF," *Atmos. Chem. Phys.*, vol. 18, no. 13, hal. 9975–10006, 2018.
[34] N. Liu, B. Zou, H. Feng, W. Wang, Y. Tang, dan Y. Liang, "Evaluation and comparison of multiangle implementation of the atmospheric correction algorithm, Dark Target, and Deep Blue aerosol products over China," *Atmos. Chem. Phys.*, vol. 19, no. 12, hal. 8243–8268, 2019.
[35] A. Di Sarra, D. Fuà, dan D. Meloni, "Estimate of surface direct radiative forcing of desert dust from atmospheric modulation of the aerosol optical depth," *Atmos. Chem. Phys.*, vol. 13, no. 11, hal. 5647–5654, 2013.
[36] A. Dementeva, G. Zhamsueva, A. Zayakhanov, dan V. Tcydypov, "Interannual and seasonal variation of optical and microphysical properties of aerosol in the Baikal region," *Atmosphere (Basel).*, vol. 13, no. 2, hal. 211, 2022.
[37] I. Koren, G. Feingold, dan L. A. Remer, "The invigoration of deep convective clouds over the Atlantic: aerosol effect, meteorology or retrieval artifact?," *Atmos. Chem. Phys.*, vol. 10, no. 18, hal. 8855–8872, 2010.